

RSC Advances



This is an *Accepted Manuscript*, which has been through the Royal Society of Chemistry peer review process and has been accepted for publication.

Accepted Manuscripts are published online shortly after acceptance, before technical editing, formatting and proof reading. Using this free service, authors can make their results available to the community, in citable form, before we publish the edited article. This *Accepted Manuscript* will be replaced by the edited, formatted and paginated article as soon as this is available.

You can find more information about *Accepted Manuscripts* in the [Information for Authors](#).

Please note that technical editing may introduce minor changes to the text and/or graphics, which may alter content. The journal's standard [Terms & Conditions](#) and the [Ethical guidelines](#) still apply. In no event shall the Royal Society of Chemistry be held responsible for any errors or omissions in this *Accepted Manuscript* or any consequences arising from the use of any information it contains.

ARTICLE

Synthesis and characterization of antimicrobial textile finishing based on Ag:ZnO nanoparticles/chitosan biocomposites

Cite this: DOI: 10.1039/x0xx00000x

Receivedth 2014,

Acceptedth2014

DOI: 10.1039/x0xx00000x

www.rsc.org/

Mariana Bușilă,^a Viorica Mușat,^{a*} Torsten Textor^b and Boris Mahltig^c

ZnO and Ag:ZnO nanoparticles were prepared by hydrolysis of zinc acetate in the presence of lithium hydroxide (LiOH). In combination with binders based on hybrid polymer sols, these metal oxide materials were applied for textile treatment. Hybrid coatings based on ZnO, Ag:ZnO/CS, Chitosan (CS), 3-glycidyloxypropyltrimethoxysilane (GPTMS) and tetraethoxysilane (TEOS) prepared by sol-gel method were applied on cotton 100% and cotton/polyester (50/50%) textiles using „pad-dry-cure” technique. The obtained nanoparticles incorporated within chitosan matrix were characterised by X-ray diffraction (XRD), Fourier transform infrared (FTIR) spectroscopy, thermogravimetric analysis (TGA), UV/Vis spectroscopy and field emission scanning electron microscopy (FE-SEM). The antimicrobial activity of Ag/CS, ZnO/CS and Ag:ZnO/CS composite coatings was investigated in comparison to that of the pure chitosan using the paper disc method on Mueller-Hinton agar, against the Gram-negative *E. coli* and the Gram-positive *S. aureus* bacteria. For the same composite coatings applied on textile, the antimicrobial activity was investigated by UV/Vis absorption spectroscopy using TTC method, against the bacteria *E. coli* and *M. luteus*. The investigated nanocomposite materials showed good antimicrobial activity and are promising materials for use as medical applications.

1. Introduction

The treatments of the textile materials for the functionalization with antibacterial finishing agents are applied in order to obtain technical materials, but also to limit their deterioration caused by mildew, especially for fabrics made from natural fibres, like cotton¹, which are more susceptible to microbial attack than synthetic fibers.² Fabrics are excellent media for the growth of microorganisms when the basic conditions such as nutrients, moisture, oxygen and appropriate temperature are met. The requirements for use of technical textiles and clothing with antimicrobial properties are currently increasing, in order to ensure a healthy and comfortable life environment for people. The care for human protection, and the rapid development of health, safety and environmental legislation led to a dynamic increase in technical textile market, like sutures, bandages, specialized wound dressings, gauze, masks, surgical gowns and hospital linen. In the industrial practice, a number of chemicals have been used to obtain antibacterial activity on textiles.^{3,4} Because many of these chemicals are toxic to humans and cannot easily degrade in the natural environment, the textile industry continues to look for eco-friendly processes that can be carried out without toxic textile chemicals.

Biomaterials like chitin and chitosan have been employed for antimicrobial purpose. Chitosan (CS) obtained complete deacetylation of chitin has one amino group and two hydroxyl groups per monomer unit and represents an attractive polymer for the encapsulation of different chemicals for textile materials treatment. This most plentiful natural biopolymer with antimicrobial activity has at the same time the advantages of biocompatibility, excellent film-forming ability and biodegradability. It is one of the compounds, among xerogels, charcoal cloth, alginates and hydrogels, used for the preparation of specialized dressing for different wounds, having a great potential in wound healing and skin burns.⁵ There is a lot of literature on the use of chitosan based antimicrobial materials for textiles, where bulk chitosan has been used as finishing coating.⁶ Wazed et al. have demonstrated the advantage of using chitosan nanoparticles (NPs) instead of bulk chitosan, in order to impart enhanced antimicrobial activity of bioactive polyester fabric, at very low concentration.⁷ Studying the application of nanochitosan for wool fabric finishing, Yang et al. concluded that the molecular weight of CS directly determines the size of chitosan nanoparticles, which in turn influences its antimicrobial activity.⁸ The combination of CS with inorganic NPs

was an efficient approach to produce antibacterial materials with improved functional properties. It has been reported that the CS-based composites with silver nanoparticles, silver zeolite or silver hydroxapatite provide increased mechanical strength and water barrier properties.^{9,10} Silver nanoparticles were among the earliest investigated inorganic nanoparticles for their antibacterial and wound healing properties, and several such products already are commercialized.¹¹⁻¹³ Products containing silver nanoparticles have the ability to exert bactericidal effects and are less harmful to human cells than other toxic organic antimicrobial agents.^{13,14}

In recent years, much effort has been devoted to the development of organic/inorganic hybrids, especially based on biopolymer and metal ions, in order to link the chelating capacity of biopolymer with the antimicrobial properties of metal ions. The chelation of chitosan-metal ion increases the positive charge density of chitosan which is expected to lead to enhanced adsorption of polycation onto the negatively charged cell surface, causing the inhibition of cell growth.^{15,16} Up to now nano-sized particles such as nano-TiO₂ were applied on textiles for self-cleaning and in hygienic textiles.^{17,18} Among the metal oxide compounds, in the last decade, ZnO NPs have attracted wide interest due to its good photocatalytic activity, high stability, nontoxicity and antibacterial properties for application in the field of cosmetics, depollution, protective medical clothes.¹⁹ Because of its anti-inflammatory, drying, mild astringent and antiseptic properties, zinc ion can play also a major role in wound healing, especially from burns.⁵ Recent studies on ZnO-CS composites in the form of films, membranes and dyes have indicated that the presence of ZnO NPs in all cases significantly improved the antibacterial properties of CS.^{20,21} The advantages of combining CS with ZnO NPs as an alternative to the widely used Ag NPs reside in their lower cost, lack of color and UV-blocking properties.²² Different methods have been reported for the preparation of ZnO-CS nanocomposites in solution^{20,21} or applied as coating on cotton.²³ Farouk et al. presented the antibacterial activity of cellulosic cotton (100%) and cotton/polyester (65/35%) fabrics treated with sol-gel hybrid polymers based on 3-glycidioxypropyltrimethoxysilane (GPTMS), ZnO nanoparticles and chitosan.² Perelshtein et al. prepared nanostructured chitosan (CS) and chitosan-ZnO complex coatings deposited on cotton fabrics using ultrasound technique.²⁴ Hebeish et al. reported the preparation of chitosan and chitosan-copper nanoparticles with different particle sizes, applied to cotton fabric using GPTMS as a cross linking agent, which enhances antibacterial and UV-protection properties.²⁵ The use of GPTMS as cross linking agent between ZnO nanoparticles and the chitosan matrix, in order to obtain the antimicrobial ZnO-CS binary composites has been also reported by Farouk et al.² A very small number of papers reports on the preparation of antimicrobial complex hybrid composites based on ZnO NPs, silver and chitosan, in the form of films deposited on glass²⁶ or finishing coating deposited on wound dressing⁵, without mentioning any functionalization agent used for dispersion of ZnO NPs.

In this study, a novel complex biocompatible antimicrobial nanocomposite coating consisting of three antimicrobial agents (Ag NPs, ZnO NPs and CS) chemically bound to each other but also on the textile fiber through two functionalization agents (GPTMS and TEOS) is presented. In addition to the literature data, in this study a

second functionalization agent (TEOS) was used for a better dispersion and a stronger binding of the nanoparticles in the CS matrix and also for a better adhesion to the textile fiber. In contrast to the data reported so far, this study investigates the antimicrobial activity of Ag:ZnO nanocomposite nanoparticles with a broader range of Ag concentrations starting at very low concentration and up to 15%, deposited as hybrid coatings in chitosan matrix on 50%-50% cotton-polyester fabrics, using „pad-dry-cure” technique. The antimicrobial activity of the obtained hybrid composite coatings was investigated using the paper disc method on Mueller-Hinton agar, against the Gram-negative *E. coli* and the Gram-positive *S. aureus* bacteria and TTC method, against *E. coli* and *M. luteus* bacteria. Photoluminescent properties of the biocompatible nanocomposite samples were highlighted. In the future these developed materials are promising for applications in the medical field, where they are used as sutures, bandages, scaffolds, wound dressing, masks, surgical gowns and hospital linen.

2. Experimental

2.1 Materials

Zinc acetate dihydrate, silver nitrate, 2-propanol and chitosan with low-molecular-weight (50kDa) and 75–85% degree of deacetylation purchased from Sigma–Aldrich Chemical Co and glacial acetic acid purchased from Beker have been used for nanoparticles and hybrid coatings preparation. Nutrient broth (Merck), nutrient agar (Merck), blanc discs (Bioanalyse) and 2,3,5–Triphenyltetrazolium chloride (Sigma–Aldrich) were used to carry out the antimicrobial testing. The deionized water was obtained from Millipore Milli-Q water purification system.

2.2 Preparation of ZnO and Ag:ZnO nanoparticles

ZnO and Ag-doped ZnO nanoparticles were prepared by hydrolysis of zinc acetate in isopropanol in the presence of lithium hydroxide (LiOH), similar to that of Spanhel method.²⁷ The 0.035M solution of (ZnAc)₂·2H₂O was prepared in 500 mL 2-propanol under reflux heating at 82°C for three hours. 0.035M lithium hydroxide solution was obtained by dissolving LiOH in 500 mL isopropanol at room temperature under vigorous magnetic stirring. For the preparation of the Ag-doped ZnO nanoparticles with different atomic ratios of 99.9:0.1, 95:5 and 85:15, adequate amounts of AgNO₃ were added in the previously prepared (ZnAc)₂·2H₂O solution. The resulting colorless solution was cooled down to 0°C before being added drop by drop the lithium hydroxide solution under vigorous stirring. The ZnO solution was stored at ≤ 4°C for 24 hours. High-speed centrifugation (4000 rpm/20 min) was used for the separation of the ZnO and Ag-doped ZnO nanoparticles from mother solution, followed by rinsing with isopropanol. Afterwards, the powders were dried at 60 °C.

2.3 Preparation of composite coatings precursors

The preparation of hybrid Ag/CS, ZnO/CS and Ag:ZnO/CS composite coatings was achieved in two stages: first, the

solution of chitosan (1 g) in 60 mL acetic acid (1%) was prepared under magnetic stirring for 24h and then ZnO, Ag:ZnO nanoparticles or AgNO₃ in solution were functionalized with GPTMS (5 mL) and TEOS (5 mL) and added to the chitosan solution (under magnetic stirring for 3h). The ethoxy and methoxy groups of TEOS and GPTMS undergo hydrolysis and condensation leading to the sol formation. When this sol is added into chitosan solution, further hydrolysis and condensation takes place forming an organic-inorganic hybrid sol. The Si-OH group of TEOS and GPTMS reacts with hydroxyl group at C-6 position of chitosan as well as condensation of two Si-OH groups forms Si-O-Si network forming polymer. The same result were reported by Brinker et al., mentioning that the hydrolysis process in sol-gel method is performed between water and silane.²⁸

The obtained liquid precursors have been applied as coating agents for textile treatment. Fig. 1 shows the proposed scheme for the preparation of ZnO, Ag:ZnO and Ag in chitosan matrix precursors, in the presence of functionalization agents, and its application to cellulosic fabrics.

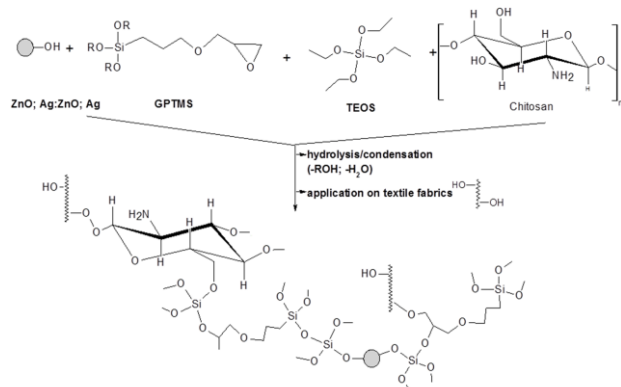


Fig. 1 Proposed scheme for the preparation of ZnO/CS, Ag:ZnO/CS and Ag/CS composite coatings

Table 1 Investigated nanocomposites coatings samples

Samples	Samples code	[Ag ⁺]
Ag:ZnO/chitosan	CS-1	0.1at%
	CS-2	5at%
	CS-3	15at%
ZnO/chitosan	CS-4	-
Ag/chitosan	CS-5	0.1at%
	CS-6	5at%
	CS-7	15at%
Chitosan – reference sample	CS-8	-

2.4 Application of composite coatings on textile fabrics

The coatings were applied on plain-weave fabrics made of scoured and bleached cotton, and on blended polyester/cotton (50/50%) fabrics with a mass per unit area of 250 g/m² and 182 g/m², respectively. Both materials are standard test materials supplied by WFK (Brüggen, Germany). The nanocomposites were applied to the fabrics by a pad-dry-cure process using a laboratory padder equipped with the roles of a standard rubber

hardness of 70° Shore (Mathis, Switzerland). The nip-pressure was adjusted to a value guaranteeing a wet pick up of 100%; the role speed was 4m/min. After padding, the samples were dried in a labcoater (Mathis, Switzerland) at 130°C for 30 min before being washed to remove the residual by-products.

2.5 Materials characterization

The crystalline structures of the obtained composites were identified by X-ray diffraction using a Bruker D8 Discover Advanced with CuK_α radiation ($\lambda = 1.542 \text{ \AA}$).

FT-IR analysis of pure chitosan and Ag:ZnO/CS, ZnO/CS, Ag/CS nanocomposites were carried out in the range between 4000 and 500 cm⁻¹ using an Agilent Cary 630 FTIR spectrometer on film obtained after drying the composite solution at 50 °C.

The morphological characteristics of the composite coatings were examined using an with high resolution Field Emission Scanning Electron Microscopy (FE-SEM), Nova NanoSEM 630, FEI Company, USA. The samples for ESEM-EDAX measurements were obtained by drying a drop of solution on the top of the carbon tape.

The thermogravimetric analysis was carried out using a TGA Q5000IR instrument, at a heating rate of 10°C/min in nitrogen atmosphere.

The UV-Vis absorbance spectra of liquid sol samples were recorded within 250-780 nm wavelength range, using a double beam ultraviolet-visible spectrophotometer PC Labomed, Inc - USA.

Photoluminescence (PL) emission spectra of the nanosol samples were recorded on Microplate reader with a fluorescence spectrometer Infinite 200 PRO NanoQuant (Tecan-Switzerland), in the 400-700 nm range, with excitation (λ_{ex}) at 365 nm.

2.6 Antimicrobial testing of sols

The antimicrobial activity of Ag/CS, ZnO/CS and Ag:ZnO/CS composite sols with respect to simple CS polymer sol was investigated by using the paper disc method on Mueller-Hinton agar against the Gram-negative bacteria, *Escherichia coli* (*E. coli*) and the Gram-positive bacteria, *Staphylococcus aureus* (*S. aureus*) on Mueller-Hinton agar with blood. Sterilized paper disc of 6 mm in diameter impregnated with 10μL (5mg/1mL) solution of the composite have been used. In each sterilized dish, 0.2 mL fresh broth cultured for 24 h followed by 20 mL melted nutrient agar medium was added at approximately 50 °C. The dishes were then cooled down to room temperature. The obtained samples were gently pressed against the medium plate to have good contact with the inoculated agar, then turned flat. The samples were kept in incubator at constant temperature at 37°C ± 1 °C for 24 h, before the inhibition zones were measured. The method used for antimicrobial testing is standardized by correlation of zone diameters with minimal inhibitory concentration determined in broth.

2.7 Antimicrobial testing of nanocomposites coatings on textile fabrics

The antimicrobial activity of hybrid composite coatings applied on textile fabrics was tested against the Gram-negative bacterium *Escherichia coli* (DSMZ 498) and Gram-positive *Micrococcus luteus* (ATCC-No. 9341) using Tetrazolium/formazan-test method (TTC). In this test, both untreated and coated fabrics were cut into small size (1g). Before incubation, the samples were sterilized at 110 °C and placed in 40 ml nutrient broth medium flask which contain 10 µl of microorganism (10^8 CFU/ml), then all flasks were incubated with shaking at 37 °C at 200 rpm for 3 h. After that, one mL of each flask containing the control and the coated samples was added to the sterilized test tubes containing 100 µL TTC (0.5 %w/v). All tubes were incubated at 37 °C for 20 min. The resulted formazan was centrifuged at 4000 rpm for 3 min followed by decantation of the supernatant. The pellets thus obtained were resuspended and centrifuged again in ethanol. The activity and viability of the cells was determined by measuring the formazan absorbance value at 480 nm using a Cary 5E-Varian UV-VIS-NIR Spectrophotometer.²⁹

3. Results and discussion

3.1 Structure and morphology

Fig. 2 shows the X-ray diffraction patterns of the investigated samples (Ag:ZnO/CS, ZnO/CS, Ag/CS composites and pure CS). More polymorph phases of chitosan are mentioned in the literature.³⁰ In the solid state, the chitosan is a semicrystalline polymer. The deacetylation, usually done in the solid state, gives an irregular structure due the semicrystalline character of the initial polymer.^{31,32} According to Trang et al., a quasi-amorphous form of chitosan has only background raised at about $2\theta = 20^\circ$; the presence of XRD peaks within the range of small angles suggests the ordering of the chitosan structure on molecular level.³³ In the XRD pattern of the simple chitosan sample (curve d in Fig. 2), the only one peak is visible at $2\theta = 22.3^\circ$, showing a quasi-amorphous structure. In the diffraction pattern of the ZnO/CS and Ag-ZnO/CS composite coatings (curves a and b in Fig 2), the chitosan peak at $2\theta = 22.3^\circ$ lowers and shifts towards lower angles and a new peak appears at $2\theta = 11.4^\circ$. For these composites, the shift of $2\theta = 22.3^\circ$ toward lower values and the presence of peaks at $2\theta = 11^\circ$ and 7° suggest the ordering on the molecular structure of the chitosan in the presence of the crystalline network of ZnO. The diffraction pattern of the Ag:ZnO/CS composites (curve a in Fig. 2) exhibits three additional small peaks at 31.8° , 34.4° and 36.5° assigned to the most important (1 0 0), (0 0 2), (1 0 1) planes of hexagonal structure of zinc oxide nanoparticles and other two peaks at 38.2° and 44.3° indicating the presence of the Ag phase.^{1,2} Values of the structural parameters $a = 5.207 \text{ \AA}$ and $c = 3.25 \text{ \AA}$ for the ZnO phase and $a = 4.086 \text{ \AA}$ for the Ag phase were calculated from XRD patterns. The same peaks at 38.2° and 44.3° appear in the diffraction pattern of the Ag/CS composite (curve c in Fig. 1) confirming the presence of the

cubic structure of the metallic Ag phase embedded in chitosan matrix. The shift at higher 2 theta angles of the diffraction peak of chitosan in the Ag/CS composite, compared to that of simple chitosan sample, can be explained by the tensions that arise in the composite network due to Ag phase incorporation.³⁴

Fig. 3 presents the FTIR spectra of the investigated samples. The FTIR spectrum of chitosan shows characteristic bands at 3303cm^{-1} attributed to the combined peaks of -NH₂ and -OH groups stretching vibration³⁵, absorption bands at 2926 and 2856 cm^{-1} attributed to asymmetric stretching of -CH₃ and -CH₂, absorption peaks at 1627 cm^{-1} ascribed to bending vibration of -NH₂ group and stretching vibration of C=O group.³⁵

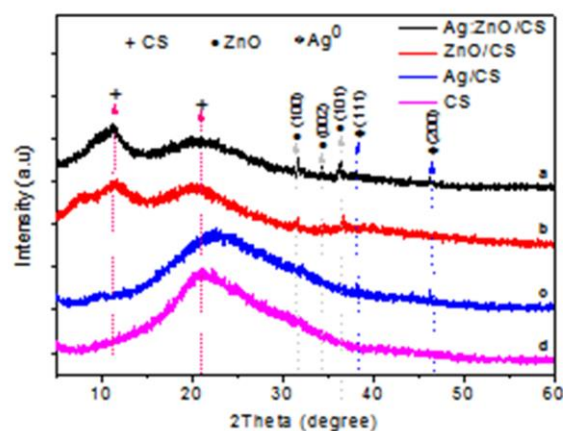


Fig. 2 XRD pattern of a) Ag:ZnO/CS (CS3), b) ZnO/CS (CS4), c) Ag/CS (CS7) composites and d) chitosan (CS8)

The bands at 1393 and 1009 cm^{-1} were attributed to the CH₃ symmetrical deformation mode and the C-O stretching vibrations (C-O-C), respectively.

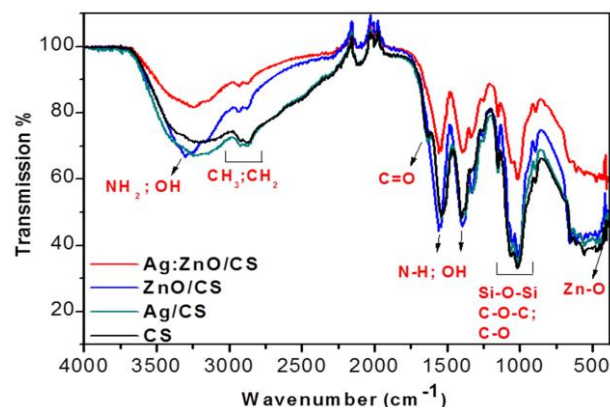


Fig. 3 FTIR Spectra of ZnO/CS (CS4), Ag:ZnO/CS (CS3), Ag/CS (CS7) and CS films (CS8)

The absorption band at 554 cm^{-1} is attributed to the stretching mode of Zn-O.³⁶

The band of chitosan-(TEOS and GPTMS) hybrid coating appearing at 2946 cm^{-1} is due to the presence of -CH₂- group of GPTMS.

The intensity of the band appearing at 1100-1000 cm^{-1} increases mostly due to overlapping of the Si-O-Si and -C-O-C- groups. The overlapping of these bands was already reported previously in the literature.³⁷ In the FTIR spectra of Ag:ZnO/CS, the bending vibration of OH group and that attributed to amino group appeared at 1538 cm^{-1} .³⁸

Generally, one can observe a superposition of the spectra of the investigated samples, but with different band broadening for Ag:ZnO/CS and ZnO/CS in the 3000-3500 cm^{-1} range. Further, a small shift of these peaks to higher wavenumber indicates, as observed from the XRD pattern, the strong attachment of ZnO to the hydroxyl, amino and amide groups of the chitosan molecules.³⁹

From the thermogravimetric analysis of the investigated samples shown in Fig. 4, different thermal events in the range of 50-500 $^{\circ}\text{C}$, with mass loss in the range of 50-62%, were observed. The DTG curves highlight three steps of the thermal process. The first step, from 50-150 $^{\circ}\text{C}$, can be attributed to the elimination of absorbed water by drying, while the next two steps are attributed to oxidative decomposition. According to some authors,⁴⁰⁻⁴² the second stage of degradation, between 150 and 250 $^{\circ}\text{C}$, is connected to the deacetylation and depolymerization of chitosan.

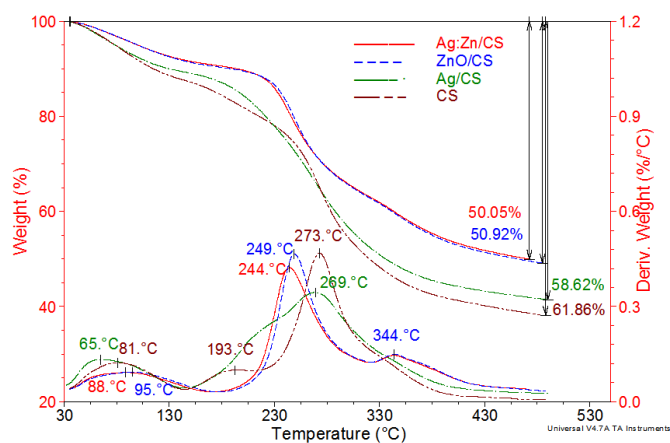


Fig. 4 TG-DTG curves for the thermal decomposition of Ag:ZnO/CS (CS3), ZnO/CS (CS4), Ag/CS (CS7) nanocomposite and pure chitosane (CS8)

The mass loss is smaller in the presence of ZnO and Ag/ZnO nanoparticles, confirming the interaction between ZnO nanoparticles and chitosan, that slows down the decomposition process, which starts with the amine groups, and leads to an unsaturated structure.³⁹

The third step, between 250 and 500 $^{\circ}\text{C}$, corresponds to the dissociation of hydrogen bonding from chitosan interchain,⁴³⁻⁴⁵ which is strongly formed among the $-\text{NH}_2$ and $-\text{OH}$ functional groups.⁴³⁻⁴⁵ The thermal parameters including the maximum temperature of the degradation and total weight loss are summarized in Table 2.

The maximum temperature of DTG peaks (Table 2), also indicates a chemical interaction of ZnO and Ag/ZnO nanoparticles with chitosan. The improvement of the thermal

stability of polysaccharide structure (CS) in the presence of ZnO and Ag/ZnO has been also observed by other researchers.⁴⁶⁻⁴⁸

Table 2 Thermal properties of Ag:ZnO/CS (CS3), ZnO/CS (CS4), Ag/CS (CS7) nanocomposite and CS pure (CS8)

Sample	T_{max} ($^{\circ}\text{C}$)			Total weight loss (%)
	Step I	Step II	Step III	
Ag:ZnO/CS	89	244	344	50
ZnO/CS	96	249	344	51
Ag/CS	65	210	269	59
CS	81	193	273	62

Fig. 5 shows the FESEM images on the surface of the films resulted by evaporation of pure CS solution and CS-based nanocomposite solutions. While the simple chitosan film displays a smooth surface (Fig. 5 d), the surface of blend films became uneven and studded with dense grains (Fig. 5 a-b). The Ag/CS film shows very small Ag nanoparticles, between 3-5 nm, dispersed in the CS matrix, and some agglomerates of silver and CS up to 20nm (Fig. 5 c).

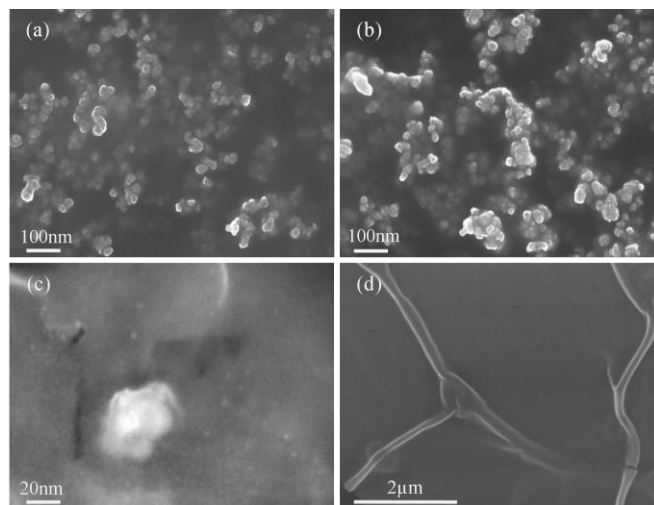


Fig. 5 FESEM images of a) Ag:ZnO/CS (CS3); b) ZnO/CS (CS4); c) Ag/CS (CS7) nanocomposite and (d) pure chitosane (CS8)

The size of Ag:ZnO and ZnO nanoparticles ranges between 10-35 nm. The composite Ag:ZnO/CS NPs display an even better dispersion and uniformity (Fig. 5a), compared to ZnO/CS, where ZnO grains shows a larger size distribution with slightly bigger agglomerates (Fig. 5b). Silver seems to play an important role on the distribution of nanoparticles within the chitosan matrix, as can be observed in Fig. 5.a.

The FESEM micrographs on the surface Ag:ZnO/CS nanocomposite coatings deposited on the textile fibers presented in Fig. 6, show both areas with a distribution of individual nanoparticles (10-30nm) (Fig. 6 e and k) and areas with groups of individual NPs or aggregates of nanocomposites NPs (Fig. 6 i and j). From the FESEM image shown in the detail in Fig. 6 d, can be observed that the Ag:ZnO/CS coating consists of Ag:ZnO composite NPs formed from very small roundish Ag quantum dots of about 10 nm in situ grown on the

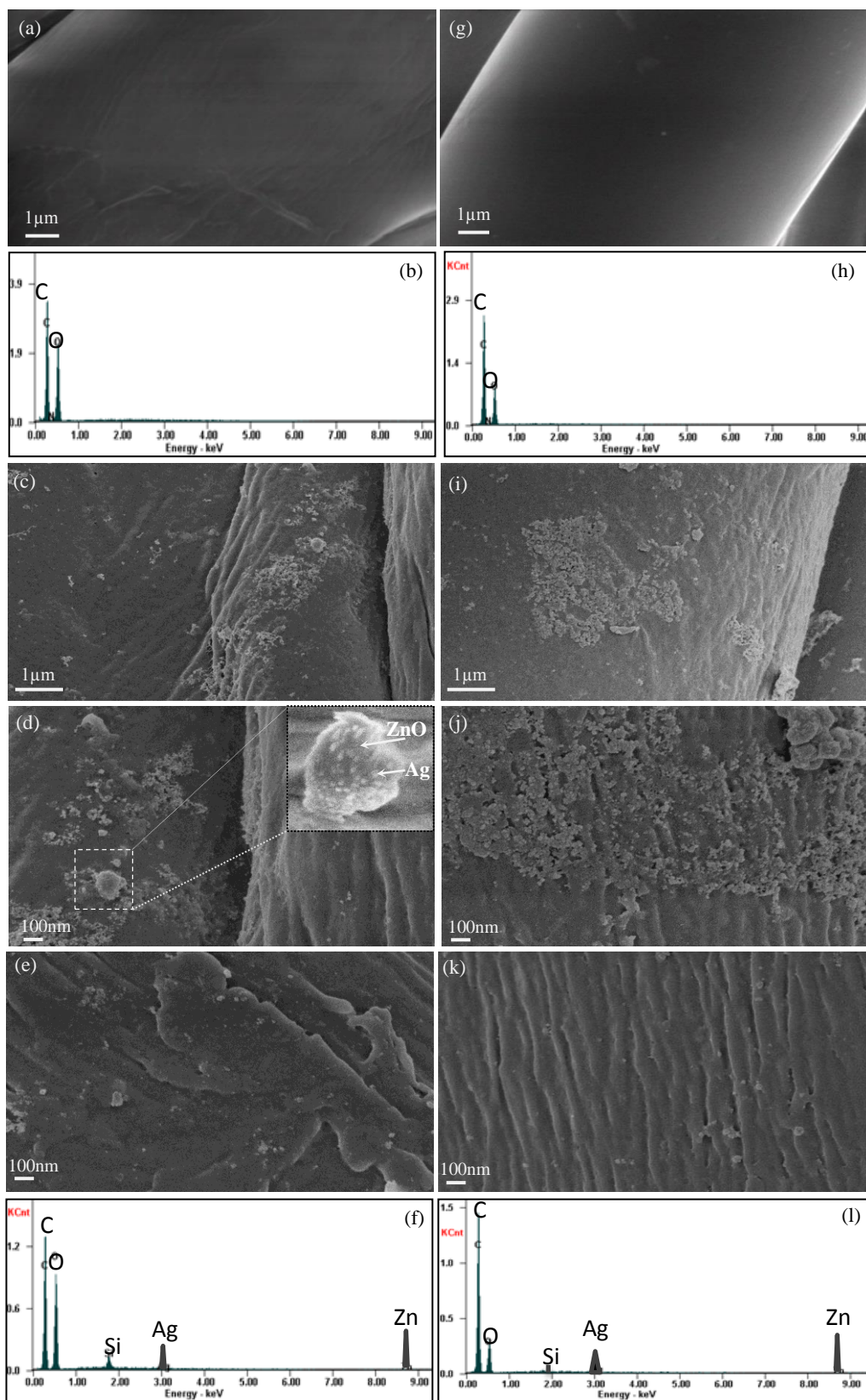


Fig. 6 FESEM images of (a, f) 100% cotton and (b-f) cotton/polyester 50/50% textiles, (g-l)

surface of polyhedral ZnO NPs.

In situ formation of Ag:ZnO/CS composite coatings also involves the embedding of these Ag:ZnO nanocomposite NPs into CS matrix. One can notice that this embedding results in a dispersion of small Ag:ZnO nanocomposite NPs (Fig. 6 e and k), along with associations of small nanocomposite NPs. Some bigger aggregates of nanocomposite NPs (Fig. 6 c-d and i-j) can also be observed.

3.2 Optical properties of sol precursors

From Figure 7 that shows the UV-Vis absorbance spectra of the investigated samples, one can notice that simple CS and Ag/CS samples show one absorption band at 319 nm and 307 nm, respectively, while ZnO/CS and Ag:ZnO/CS samples exhibit two absorption bands each, at 301 and 420 nm and at 308 and 417 nm, respectively. Comparing the spectra of the last two samples with those of the first two ones, it can be appreciated that the peak at about 319 nm is given by chitosan, while the peaks at about 367 and 420 nm corresponds to silver NPs⁵¹ and ZnO.^{49,50}

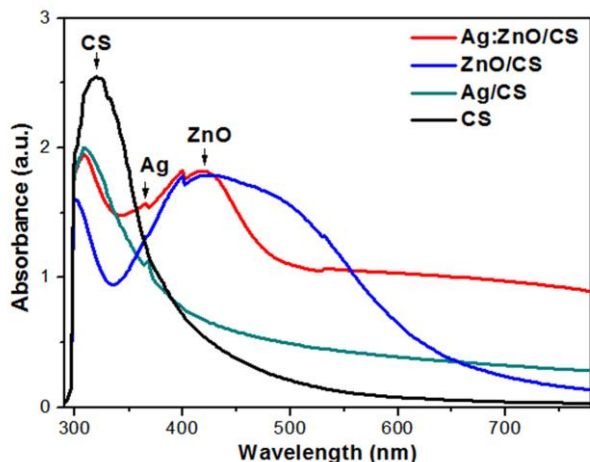


Fig. 7 UV-VIS absorbance spectra of Ag:ZnO/CS (CS3), ZnO/CS (CS4), Ag/CS (CS7) nanocomposite and pure chitosane (CS8)

In the case of the biocomposite samples, a lower intensity and a blue-shift of the chitosan peak were observed, indicating that Ag and ZnO within chitosan matrix are in the size of nanometer, which is consistent with the SEM images. Similar behaviour was reported by others authors.⁵²⁻⁵⁴

A particular attention has been paid to the investigation of the emission spectra and fluorescent intensity of ZnO/CS, Ag:ZnO/CS and Ag/CS nanocomposite compared to pure CS. A qualitative comparison of the photoluminescence (PL) spectra for all samples is shown in Fig. 8.

The photoluminescence spectrum of the chitosan film is characterized by a maximum emission band at 423 nm. With the introduction of ZnO nanoparticles into chitosan matrix the emission increases, as illustrated in Fig. 8 b (sample 2) and d (sample 2).

These highly luminescent, nontoxic and biofriendly ZnO nanoparticles in chitosan matrix, have exciting application potential as fluorescent probes in biomedical applications by easily attaching biomolecules to the bare surface of these composites.

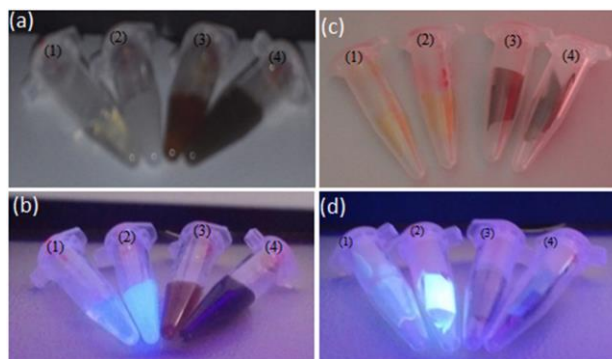
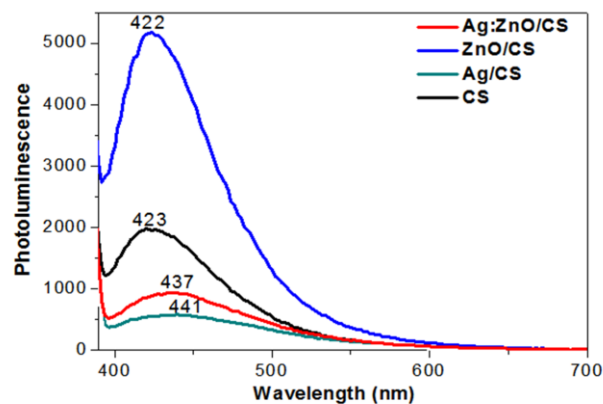


Fig. 8 Top: Photoluminescence (PL) spectra of ZnO/CS (CS4), Ag:ZnO/CS (CS3), Ag/CS (CS7) nanocomposites and pure CS (CS8). Down: Digital photos in the absence (a and c) and presence (b and d) of UV light of ZnO/CS (2), Ag:ZnO/CS (3) and Ag/CS (4) nanocomposites compared with pure CS (1); in solution (a and b) and films (c and d).

After the introduction of Ag into the chitosan matrix the emission is still present, but it decreases with increasing silver concentration within nanocomposite matrix. Higher silver concentration, lowers the intensity of the emission and leads to a red shift. Since the silver produces absorption bands in the region of chitosan emission, the observed decrease can be attributed to a non-radiative energy transfer mechanism such as charge transfer. This decrease in the photoluminescence could be a consequence of the overlap between the absorption band of Ag and the emission band of chitosan.^{48,55} It can be concluded that Ag doping lowers the emission intensity, while ZnO doping enhances it.

3.3 Antibacterial activity of sol precursors

Fig. 9 shows the antimicrobial activity of the investigated nanocomposite sols with different concentration of Ag (as shown in Table 1) compared to simple CS (CS8) solution. The sols impregnated in the disk paper placed on the bacteria-inoculated

surfaces killed most of the bacteria under and around them, generating distinct zones of inhibition (clear areas with no bacterial growth) around them, both for *E. coli* and *S. aureus* bacteria. At equal Ag concentration, Ag:ZnO/CS nanocomposite samples (CS1-2-3) have a slightly higher antimicrobial activity than Ag-CS nanocomposite samples (CS5-6-7).

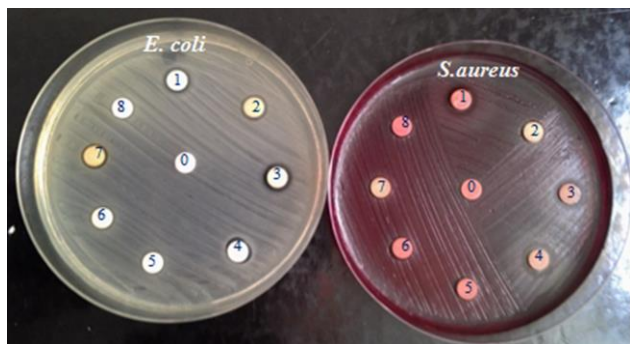


Fig. 9 Inhibition zone of 1) ZnO/CS (CS4); 2) Ag:ZnO/CS (CS1); 3) Ag:ZnO/CS (CS2); 4) Ag:ZnO/CS (CS3); 5) Ag/CS (CS5); 6) Ag/CS (CS6); 7) Ag /CS (CS7) and pure CS (CS8)

The chitosan, which is positively charged, interacts with the strongly electronegative lipidic bacterial membranes, changing their permeability and affecting the cell growth and viability.^{24,60,61} The local association, at nanoscale, of these mechanisms produces the synergistic enhancement of the antibacterial activity.

3.4 Antibacterial activity of coated fabrics

The results of the quantitative evaluation of ZnO/CS, Ag:ZnO/CS, Ag/CS and CS nanocomposite coatings applied on cotton and cotton/polyester, using TTC method are presented in Fig. 10. This shows the viability reduction of *E. coli* and *M. luteus* in the presence of these nanocomposite coatings. As mentioned in the experimental section, the viability is measured based on concentration of formazan that is formed in the presence of vital microorganisms, so that it is directly proportional to the amount of living bacteria. The obtained data are in good agreement with the results of the qualitative investigation shown before. All samples exhibit antimicrobial activity with a degree of reduction of the bacterial viability index 50%.

The TTC test of antimicrobial activities (Fig. 10) shows that 5-15% Ag-doped ZnO/CS biocomposites have higher antimicrobial activity than ZnO/CS and 5-15% Ag/CS biocomposites, and more interesting, higher than the cumulative activity of the two components (Ag and ZnO) in chitosan matrix, for the same Ag concentration, indicating the synergistic effect of Ag NPs and ZnO NPs. The observed results could be explained by local association, at nanoscale, of different mechanisms discussed in literature⁵⁶⁻⁵⁹, by which Ag, ZnO and CS acts on the microbial cell. Ag disturbs the permeability, respiration and cell division, based on the following mechanisms: silver ions attach to proteins and neutralize them, interact with the microbial membrane to cause structural and permeability changes and interact with microbial nucleic acids to

inhibit microbial replication. In the light and the presence of transition metals, Ag improved the charge transfer, reducing the chance of electron-hole pairs to recombine and promoting the generation of perhydroxyl radicals and other strong oxidizing radicals.^{56,57} ZnO NPs acts through the following mechanisms: bacterial attachment by electrostatic interaction and generation of reactive oxygen species (ROS), which leads to membrane disruption, and finally to bacteria inhibition.^{58,59} Ongoing experiments are carried out in future to prove the synergistic effect of combining these different antimicrobial mechanisms.

Antimicrobial activity increases with increasing the Ag-doping in Ag:ZnO nanoparticles dispersed in chitosan matrix (CS1-CS3).

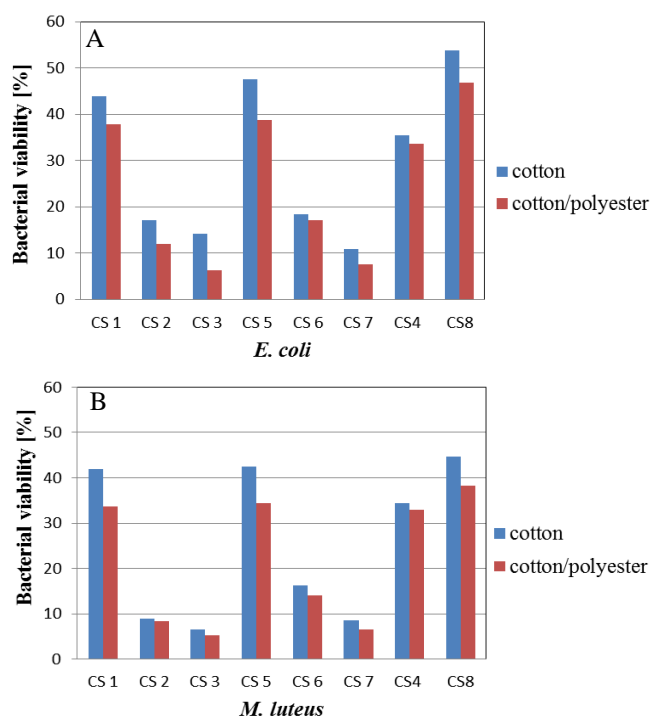


Fig. 10 Antimicrobial activity of Ag:ZnO/CS (CS1-CS3), ZnO/CS (CS4), Ag/CS (CS5-CS7) nanocomposites and CS (CS8), applied on cotton and cotton/polyester against *E. coli* (A) and *M. luteus* (B) bacteria

Fig. 10 B presents the bacterial viability of *M. luteus* bacteria in the presence of composites coating applied on cotton and cotton/polyester fabrics.

It can be observed the same trend as in the case of *E. coli* bacteria, that is, the bacterial viability decreases with increasing Ag-doping ZnO nanoparticles embedded in the matrix of chitosan, with a higher degree of inhibition of the *M. luteus* bacteria.

In the same way, the antimicrobial potential is more important for the Gram-positive *M. luteus* bacteria, in comparison to the Gram-negative *E. coli* bacteria. The different behavior can be attributed to differences in the composition and structure of the cell walls of the two types of bacteria. The cell wall of Gram-negative bacteria is composed of lipids, proteins and

lipopolysaccharides (LPS), which provides an efficient protection against harmful effects of chemical biocides, in contrast to Gram-positive bacterial wall.⁶²

Even a significant reduction in the viability of the bacterial species can be observed in the presence of all the investigated samples, the most advanced reduction was observed in the case of composite coatings applied on the cotton/polyester (50/50%) fiber. A different amount of 4.37g/m² and 3.54 g/m² coating composites was measured as deposited on cotton and cotton/polyester fabrics, respectively. This is due to wettability and capillary effects based on the different interactions of the coating solution with different functional groups and various porosities of the fabrics. The fact that in the case of cotton fabric the antimicrobial activity is lower than in the case of cotton/polyester, even if a greater amount of composite coating was absorbed, could be explained by lower amount of nanoparticles on the surface of porous cotton fiber. The porosity of the pure cotton fibers allows a higher amount of particles entering in the pores of the fibers, and so, smaller amount of particles remaining on the fiber surface, which leads to lower contact of Ag:ZnO nanoparticles with the bacteria.⁶²

4. Conclusions

ZnO/CS, Ag/CS and Ag:ZnO/CS nanocomposite coatings were prepared by modified sol-gel method using GPTMS and TEOS as functionalization agents and were applied to textile fabrics as antimicrobial treatment. FTIR spectra reveal chemical interactions between Ag and ZnO nanoparticles dispersed in chitosan matrix and confirm the attachment of siloxane moieties to chitosan due to the formation of a siloxane-polymer network. The resulted hybrid composite materials exhibit higher thermal stability than chitosan.

Ag-doped ZnO nanoparticles with smaller agglomeration than ZnO nanoparticles, show a better dispersion in chitosan matrix. The presence of crystalline ZnO phase in composite coatings leads to the ordering of the molecular structure of chitosan. Unlike Ag, in situ generation of zinc oxide nanocrystallites have produced an ordering of chitosan structure and a consistent increase of photoluminescence emission at 423 nm.

All samples exhibit good and very good antimicrobial activity with the ability to reduce up to 50-95% the viability of bacteria. The antimicrobial activity test showed that Ag-doped ZnO nanoparticles prepared from solution of zinc acetate and embedded in chitosan matrix has higher antimicrobial activity than both Ag/CS and ZnO/CS composite coatings. For all samples, a significant reduction in the viability of the bacteria was observed. Ongoing experiments are carried out in future to prove the synergic enhancement by local association, at nanoscale, of different antimicrobial mechanisms promoted by Ag, ZnO and CS.

The most advanced effect was observed in the case of composite coatings applied on the blended textile from cotton/polyester (50/50%). At the same time, the antimicrobial activity is higher for Gram-positive bacteria *M. luteus* than for the Gram-negative bacteria *E. coli*. Significant improvement for antibacterial properties has been obtained for cellulosic fabric.

Biocompatible, eco-friendly and low cost Ag:ZnO/CS composite coatings are strongly recommended as antimicrobial materials with potential applications in medical materials to prevent infection, particularly during the healing of wounds and burns, but also in food industry as packaging.

Acknowledgements

The authors acknowledge Prof. Dr. eng. Anca Duță from Transilvania University of Brasov - Renewable Energy Systems and Recycling Laboratory for XRD measurements, Dr. phys. Adrian Dinescu from IMT Bucharest for FESEM images and Prof. Dr. chem. Rodica Dinică from “Dunărea de Jos” University of Galați for UV-VIS spectra.

Notes and references

^a Centre of Nanostructures and Functional Materials-CNMF, “Dunărea de Jos” University of Galați, 111 Domnească Street, 800201, Galați, Romania.

E-mail: viorica.musat@ugal.ro. Tel: +40-757070613.

^b Deutsches Textilforschungszentrum Nord-West gGmbH (DTNW), Adlerstr.1, 47798 Krefeld, Germany and CENIDE, Center for Nanointegration Duisburg-Essen.

^c University of Applied Sciences, Faculty of Textile and Clothing Technology, Webschulstr. 31, 41065 Mönchengladbach, Germany.

† Footnotes should appear here. These might include comments relevant to but not central to the matter under discussion, limited experimental and spectral data, and crystallographic data.

Electronic Supplementary Information (ESI) available: [details of any supplementary information available should be included here]. See DOI: 10.1039/b000000x

- 1 Y. Gao and R. Cranston, *Text. Res. J.* 2008, **78**, 60.
- 2 A. Farouk, S. Moussa, M. Ulbricht, E. Schollmeyer and T. Textor, *Text. Res. J.*, 2014, **84**(1), 40.
- 3 S.H. Lim and S.M. Hudson, *Carbohydr. Polym.*, 2004a, **56**, 227.
- 4 S.H. Lim and S.M. Hudson, *Carbohydr. Res.*, 2004b, **339**, 313.
- 5 M. Abbasipour, M. Mirjalili, R. Khajavi and M. M. Majidi, *J Eng Fiber Fabr.*, 2014, **9**(1), 124.
- 6 M. Joshi, S.W. Ali, R. Purwar and S. Rajendran, *Indian J. Fibre Text. Res.*, 2009, **34**, 295.
- 7 S. Wazed Ali, M. Joshi and S. Rajendran, *AATCC Rev.*, ISSN:1532-8813, 2011, **11**, 49.
- 8 H.C. Yang, W.H.Wang, K.S. Huang and M. H. Hon, *Carbohydr. Polym.*, 2010, **79**, 176.
- 9 J.W. Rhim, S.I. Hong, H.M. Park and P. Y. W. Ng, *J. Agric. Food Chem.*, 2006, **54**, 5814.
- 10 S. Saravanan, S. Nethala, S. Pattnaik, A. Tripathi, A. Moorthi and N. Selvamurugan, *Int. J. Biol. Macromol.*, 2011, **49**, 188.
- 11 R. Dastjerdi, M.R.M. Mojtahedi and A.M. Shoshtari, *Macromol Res.*, 2009, **17**, 378.
- 12 R. Dastjerdi, M. Montazer, *Colloid Surface B.*, 2010, **79**, 5.
- 13 J. Tiam, K. K. Y. Wong, C. M. Ho, C. N. Lok, W.Y. Yu, C.M. Che, J.F. Chiu and P. K. H. Tam, *ChemMedChem.*, 2007, **2**, 129.
- 14 Z. Hu, W. Lai and Y. Shan, *J. Appl. Polym. Sci.*, 2008, **108**; 52.

- 15 E.I. Rabea, M.E.T. Badawy, C.V. Stevens, G. Smagge and W. Steurbaut, *Biomacromolecules*, 2003, **4**, 1457.
- 16 M. Kong, X.G. Chen, C.S. Liu, C.G. Liu, X.H. Meng and L.J. Yu, *Colloid. Surface. B.*, 2008, **65**, 197.
- 17 B. Fei, Z. Deng, J.H. Xin, Y. Zhang and G. Pang, *Nanotechnology.*, 2006, **17**, 1927.
- 18 Z.L. Shi, K.G. Neoh and E.T. Kang, *Biomaterials*, 2005, **26**, 501.
- 19 S.H. Choi, Y.P. Zhang, A. Gopalan, K.P. Lee and H.D. Kang, *Colloid. Surface A.*, 2005, **256**, 165.
- 20 L.H. Li, J.C. Deng, H.R. Deng, Z.L. Liu and L. Xin, *Carbohydr. Res.*, 2010, **345**, 994.
- 21 R. Salehi, M. Arami, N. M. Mahmoodi, H. Bahrami and S. Khorramfar, *Colloids Surf., B*, 2010, **80**, 86.
- 22 A. El. Shafei and A. Abou-Okeil, *Carbohydr. Polym.*, 2011, **83**, 920.
- 23 A. Becheri, M. Durr, P. L. Nostro and P. Baglioni, *J. Nanopart. Res.*, 2008, **10**, 679.
- 24 I. Perelshtein, E. Ruderman, N. Perkas, T. Tzanov, J. Beddow, E. Joyce, T. J. Mason, M. Blanes, K. Mollá, A. Patlolla, A.I. Frenkele and A. Gedanken, *J. Mater. Chem. B*, 2013, **1**, 1968.
- 25 A. Hebeish, S. Sharaf, A. Farouk, *Int. J. Biol. Macromol.*, 2013, **60**, 10.
- 26 L.H. Li, J.C. Deng, H.R. Deng, Z.L. Liu and X.L. Li, *Chem. Eng. J.*, 2010, **160**, 378.
- 27 L. Spanhel, M.A. Anderson, *Am. Chem. Soc.*, 1991, **113**, 2826.
- 28 J. Brinker, G.W. Scherer, *Sol–Gel Science: The Physics and Chemistry of Sol–Gel Processing*, Academic Press, NY, USA, 1990.
- 29 E. Seidler, Gustav Fischer Verlag, New York, 1991.
- 30 N. Cartier, A. Domard and H. Chanzy, *Int J. Biol. Macromol.*, 1990, **12**, 289.
- 31 M. Rinaudo, G. Pavlov and J. Desbrie`res, *Polymer.*, 1999, **40**, 7029.
- 32 M. Rinaudo, G. Pavlov and J. Desbrie`res, *Int J Polym Anal Charact.*, 1999, **5**, 267.
- 33 Z.F. Dong, Y.M. Du, L.H. Fan, Y. Wen, H. Liu and X.H. Wang, *J. Funct. Polym.*, 2004, **17**, 61.
- 34 M. Guo, P. Diao and S. Cai, *J. Solid State Chem.*, 2005, **17(86)**, 1864.
- 35 P. Bhadra, M. K. Mitra, G. C. Das, R. Dey and S. Mukherjee, *Mater. Sci. Eng. C*, 2011, **31(5)**, 929.
- 36 J.T. Yeh, C.L. Chen and K.S. Huang, *Mater. Lett.*, 2007, **61**, 1292.
- 37 R. Salehi, M. Arami, N. M. Mahmoodi, H. Bahrami and S. Khorramfar, *Colloids Surf. B.*, 2010, **1**, 86.
- 38 X. Qu, A. Wirsén and A. Albertsson, *Polymer.*, 2000, **41**, 4841.
- 39 T. Wanjun, W. Cunxin and C. Donghua, *Polymer Degrad. Stabil.*, 2005, **87**, 389.
- 40 D. De Britto and S.P. Campana-Filho, *Thermochim. Acta*, 2007, **465**, 73.
- 41 F. A. Lopez, A.L.R. Merce, F.J. Alguacil and A. Lopez-Delgado, *J. Therm. Anal. Cal.*, 2008, **91(2)**, 633.
- 42 M. Zeng, Z. Fang and C. Xu, *J. Membr. Sci.*, 2004, **230**, 175.
- 43 W. Y. Chuang, T. H. Young, C. H. Yao and W. Y. Chiu, *Biomaterials.*, 1999, **20**, 1479.
- 44 D.S. Vicentini, A.S. Mauro Jr. and C.M. Laranjeira, *Mater. Sci. Eng. C*, 2010, **30**, 503.
- 45 Y. Haldorai and J.J. Shim, *Compos. Interfaces*, 2013, **20**, 365.
- 46 B. Kilic, D. Omay, E. Kosa, L. Trabzon and H. Kizil, *J. Mater. Sci. Eng. A.*, 2012, **2(12)**, 761.
- 47 M. Beltramini and K. Lerch, *The Coordination Chemistry of Metalloenzymes*, Boston, 1982, 236.
- 48 S. Kumar, J. Dutta and P.K. Dutta, *J. Macromol. Sci. Pure Appl. Chem.*, 2009, **46**, 1095.
- 49 Z.A. Khorsand, M.E. Abrishami, W.H.A. Majid, R. Yousefi, S.M. Hosseini, *Ceram. Int.*, 2011, **37**, 393.
- 50 S. Azizi, M.B. Ahmad, F. Namvar, R. Mohamad, *Mater Lett.*, 2014, **116**, 275.
- 51 P. Mulvaney, *Langmuir.*, 1996, **12**, 788.
- 52 J.C. Xu, W.M. Liu, H.L. Li, *Mater Sci Eng C.*, 2005, **25**, 444.
- 53 P. Kannusamy, T. Sivalingam, *Polym Degrad Stabil.*, 2013, **98**, 988.
- 54 A. B. Jasso-Salcedo, G. Palestino, V. A. Escobar-Barrios, *J. Cat.* 2014, **318**, 170.
- 55 J. R. Morones, J. L. Elechiguerra, A. Camacho, K. Holt, J. B. Kouri, J.T. Ramirez and M. J. Yacaman, *Nanotechnology*, 2005, **16**, 2346.
- 56 A. Sclafani, M. Mozzanega, P. Pichat, *J. Photochem. Photobiol. A*, 1991, **59**, 181.
- 57 G. Zhou, J.C. Deng, *Mater. Sci. Semicond. Process.*, 2007, **10**, 90.
- 58 K. Feris, C. Otto, J. Tinker, D. Wingett, A. Punnoose, A. Thurber, M. Kongara, M. Sabetian, B. Quinn, C. Hanna and David Pink, *Langmuir*, 2010, **26**, 4429.
- 59 M. Ibănescu (Buşilă), V. Muşat, T. Textor, V. Badilita and B. Mahltig, *J. Alloys Compd.*, 2014, **610**, 244.
- 60 R. Brayner, R. Ferrari-Iliou, N. Brivois, S. Djediat, M.F. Benedetti and F. Fiévet, *Nano Lett.* 2006, **6**, 866.
- 61 S.W. Fang, C.F. Li, D.Y.C. Shih, *J. Food Prot.*, 1994, **57**, 136.
- 62 Q.L. Feng, J. Wu, G.Q. Chen, F.Z. Cui, T.N. Kim and J.O. Kim, *J. Biomed. Mater. Res.*, 2000, **52(4)**, 662.